DOI: 10.48011/asba.v2i1.1112

DC-DC MICRO-CONVERTER PHOTOVOLTAIC TOPOLOGY WITH SENSORS SUPPRESSION

Douglas Ohf*, Tiago Dezuo*, Bárbara A. de Sá*

*Electrical Engineering Department, Santa Catarina State University, Joinville/SC, Brazil.

Emails: douglas_ohf@hotmail.com, tiago.dezuo@udesc.br, bah.azevedo99@gmail.com

Abstract— This paper presents a novel system architecture intended to improve the cost-efficiency of DC micro-converter topologies by reducing the number of local sensors and centralizing the MPPT and control strategies to a single microprocessor. The first idea is to locally measure only the sensors required by the control, as it runs intermittently and needs a fast response for stability, and to use control techniques that naturally require less sensors. Second, we propose an MPPT strategy that relies on measuring the global power generated, by only acquiring the current reaching the DC link or battery and updating the operating point of each module one at a time. A problem that occurs when sequentially updating the modules is the possibility of power drop in a panel that is far from being re-updated, which may also lead to wrong conclusions about the module being currently updated. For that we also propose a method for detecting power drops and momentarily establishing a priority queue. The advantages of the proposed method are illustrated through numerical simulations.

Keywords— Photovoltaic systems, Sensing reduction, Micro-converters, Centralized control.

Resumo— Este artigo apresenta uma nova arquitetura de sistema fotovoltaico destinada a melhorar a relação custo-benefício das topologias com microconversores CC, reduzindo o número de sensores locais e centralizando o MPPT e as estratégias de controle em um único microprocessador. A primeira ideia é ter sensores locais apenas para medições exigidas pelo controlador, pois este é executado de forma intermitente e precisa de uma resposta rápida para estabilidade, além de usar técnicas de controle que naturalmente exigem menos sensores. Segundo, é proposta uma estratégia MPPT que se baseia na medição da energia global gerada, adquirindo apenas a corrente que atinge o *link* CC ou a bateria e atualizando o ponto de operação de cada módulo, um de cada vez. Um problema que ocorre durante a atualização sequencial dos módulos é a possibilidade de queda da geração em um painel que está longe de ser atualizado, o que também pode levar a conclusões erradas sobre o módulo que está sendo atualizado no momento. Para isso, também propomos um método para detectar quedas de potência gerada e estabelecer momentaneamente uma fila de prioridade. As vantagens do método proposto são ilustradas através de simulações numéricas.

Palavras-chave— Sistemas fotovoltaicos, Sensoriamento reduzido, Micro-conversores, Controle centralizado.

1 Introdução

Renewable energy systems have experienced an expressive growth during the past years due to the continuously rising demand for energy, environmental awareness and the inevitable upcoming scarcity of fossil fuels. In this scenario, the contribution of Photovoltaic (PV) is noteworthy, reaching a 509 GW of installed capacity worldwide in 2018, which represents a more than 25% increase from the previous year (SolarPower Europe, 2019).

Among the biggest challenges for a better cost-benefit of photovoltaic generation is the increase in the efficiency of the system. Even though the efficiency of converting solar energy into electricity of 47% by PV cells has been achieved under controlled laboratory environments (NREL, 2020), commercial modules still have an average yield in the range of 15 to 20%. Hence, it is extremely important to harness the most of the energy that can be generated. This is done mainly through the development of Maximum Power Point Tracking (MPPT) techniques (Soualmia and Chenni, 2016) and more efficient converter topologies.

In the most common topologies all the PV modules or strings of modules are interconnected to a single converter stage, typically divided into a DC-DC converter responsible for the MPPT and a DC-AC (inverter) for distribution and power factor correction. Although, several adversities arise for this configuration under non-uniform conditions. For instance, the power curve may present multiple maxima, requiring more advanced strategies for tracking the global maximum. Also, the overall generation tends to be inferior to the energy available as, with a single converter, it is not possible to regulate all modules to their optimal operation (Squersato et al., 2019). These non-uniform conditions are very common and can be caused by panels with different ages, inclinations, interconnections between the panels and irradiation levels, specially in the urban environment (Freitas et al., 2015).

The problems caused by non-uniform conditions are eliminated by the use of decentralized topologies (Cao et al., 2015). In this case, there is no compromise due to interconnected modules sharing the same operation point, which may not be optimal for all panels simultaneously under non-uniform conditions. This is the case for structures containing modules equipped with micro-inverters, which have gained market space, being characterized mainly as a "plug and play" device and presenting high efficiency, reliability and a

longer useful life (Torres, 2016). This architecture allows reaching the global maximum energy harnessing as an individual MPPT is performed for each module. However, this topologies have a higher installation cost because of the number of converters, sensors and microprocessors typically required. Moreover, for off-grid systems, multiple parallel connected AC outputs may require an additional synchronization strategy.

A possible way to retain the advantages of both architectures is to centralize the inverter function, but construct PV panel-level DC-DC micro-converters which optimize the panel output and condition the power for the inverter (York Jr, 2013). This solution results in an inverter economy, although the number of local sensors and microprocessors for the micro-converter is still high. Usually, different variables need to be measured for the MPPT strategy and for the converter control technique. The current literature presents some attempts to reduce the number of sensors as, for instance, (Seo et al., 2014) which uses estimators for the local currents, but strongly relying on the micro-converter and PV array parameters, still measuring all the local voltages and performing local control computing.

This paper presents a novel system architecture intended to improve the cost-efficiency of DC micro-converter topologies by reducing the number of local sensors and centralizing the MPPT and control strategies to a single microprocessor. The first idea is to locally measure only the sensors required by the control, as it runs intermittently and needs a fast response for stability, and to use control techniques that naturally require less sensors. Second, we propose an MPPT strategy that relies on measuring the global power generated, by only measuring the current reaching the DC link or battery and updating the operating point of each module one at a time. A problem that occurs when sequentially updating the modules is the possibility of power drop in a panel that is far from being re-updated, which may also lead to wrong conclusions about the module being currently updated. For that we also propose a method for detecting power drops and momentarily establishing a priority queue. The advantages of the proposed method are illustrated through numerical simulations.

The paper is organized as follows. This section ends with the base functions and symbols used in the paper. The next section is devoted to characterize PV systems and MPPT techniques. Section 3 presents some common topologies. The proposed micro-converter architecture, control strategy and reduced sensing algorithm are presented in the Section 4. Numerical simulations illustrate the results in Section 5 and some concluding remarks end the paper.

Base Functions. $\textsc{Ones}(\cdot)$ returns a vector of ones with the dimension specified in $(\cdot)$. $\textsc{Zeros}(\cdot)$ returns a vector of zeros with the dimension specified in $(\cdot)$. $\textsc{IndexMax}(\cdot)$ returns the index of the element with maximum value for a vector in $(\cdot)$.

Symbols. R_s - Series resistance of the PV module; R_p - Shunt resistance of the PV module; ϵ - Electron charge (1.6×10^{-19} C); η - Diode quality factor; κ - Boltzmann constant (1.38×10^{-23} J/K); T_r - Standard Test Conditions (STC) temperature (298K, i.e. 25°C); G_r - STC Irradiation (1000 W/m^2); I_{sc} - PV module short-circuit current at STC; V_{oc} - PV module open-circuit voltage at STC; γ - Temperature coefficient of I_{sc}; E_g - Band gap for silicon (1.1 eV); N_s - Number of PV cells in series in each module.

2 Photovoltaic systems

Photovoltaic modules are composed of a set of solar cells, typically connected in series, which convert sunlight energy directly into electrical energy (Casaro, 2009). Consider a module composed of N_s cells in series, whose temperature is T, receiving an irradiation G. This device may be modeled as current-controlled voltage source, where the voltage V_{pv} and the current I_{pv} at its terminals are related through the nonlinear function (Casaro, 2009), with all variables expressed in SI units,

$$0 = I_{ph} - \left(1 + \frac{R_s}{R_p}\right) I_{pv} - \frac{V_{pv}}{R_p N_s} - I_r \left(\exp\left(\frac{\epsilon}{\eta \kappa T}\left(\frac{V_{pv}}{N_s} + R_s I_{pv}\right)\right) - 1\right), \quad (1)$$

where

$$I_{ph} = \left(I_{sc} + \gamma\left(T - T_r\right)\right)\frac{G}{G_r} \quad (2)$$

$$I_r = I_{rr}\left(\frac{T}{T_r}\right)^3 \exp\left(\frac{\epsilon E_g}{\eta \kappa}\left(\frac{1}{T_r} - \frac{1}{T}\right)\right) \quad (3)$$

$$I_{rr} = \frac{I_{sc} - \dfrac{V_{oc}}{R_p}}{\exp\left(\dfrac{\epsilon V_{oc}}{\eta \kappa T_r}\right) - 1}. \quad (4)$$

From the Current-Voltage ($I - V$) characteristic in Equation (1), note there are several parameters affecting the energy generation in a solar panel. Constructive features, such as area, quality of the junction and electrical resistance, result in different characteristics for different panels. Operation conditions, such as irradiation and temperature, play a more instantaneous and often unpredictable influence on the $I - V$ characteristics.

The Figure 1(a) shows the $I-V$ characteristic curves for the polycrystalline module KC200GT from Kyocera under different irradiation values with a constant 25° temperature. The parameters of this module in Standard Test Conditions (STC[1]) are presented in Table 1 (Casaro, 2009).

[1] $T = 25$ °C and $G = 1000$ W/m^2.

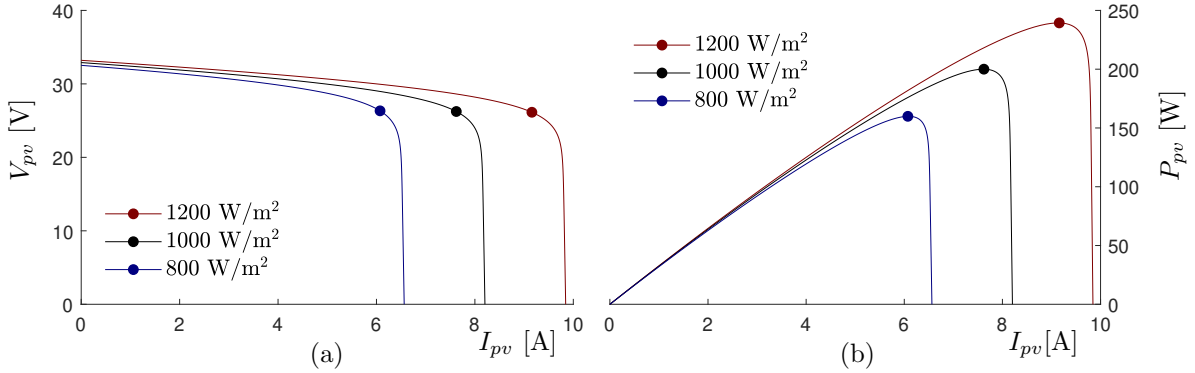

Figure 1: (a) I-V curves and (b) P-I curves for different irradiations. The symbol • denotes each MPP.

Table 1: Parameters of the KC200GT module.

Parameter	Value
V_{oc}	32.9 V
I_{sc}	8.21 A
γ	3.18×10^{-3} A/°C
η	1.2
R_s	5×10^{-3} Ω
R_p	7 Ω
N_s	54

The power generated by the PV module is given by $P_{pv} = I_{pv}V_{pv}$, resulting in the Power-Current (P-I) characteristics shown in Figure 1(b). Notice that the Maximum Power Point (MPP) changes according to the operation conditions. The literature is rich on algorithms designed to track the MPP. These MPPT are heuristics differing in terms of complexity, cost, efficiency, implementation, hardware, among others (Soualmia and Chenni, 2016).

One of the most applied MPPT techniques, due to its simplicity and efficacy, is the one known as Perturb and Observe (P&O). This method is based on analyzing the power characteristic curve in Figure 1(b) by perturbing I_{pv} or V_{pv} and observing the behavior of the generated power P_{pv}. For instance, if I_{pv} is incremented (or decremented) by a value ΔI and P_{pv} increases, then repeat the variation. Otherwise, change direction. The P&O with I_{pv} as the adjustment variable is illustrated in the Algorithm 1, where I_{ref} is the reference value to be imposed to I_{pv}.

According to the Algorithm 1, the values of V_{pv} and I_{pv} are read at a given time for the calculation of P_{pv}. This power is compared with the power stored from the previous iteration (P^*_{pv}). If they are the same, the algorithm does not make any changes. If they are different, it is verified whether the power increased or decreased and what was the direction of the last variation imposed on the current.

Algorithm 1 Traditional Perturb & Observe

Require: V_{pv}, I_{pv}
Ensure: I_{ref}
Data: ΔI
Initialize: $I_{ref} \leftarrow \Delta I$, $I^*_{pv} \leftarrow 0$, $P^*_{pv} \leftarrow 0$

```
loop
    P_pv ← V_pv I_pv
    if (P_pv − P*_pv)(I_pv − I*_pv) > 0 then
        I_ref ← I_ref + ΔI
    else
        I_ref ← I_ref − ΔI
    I*_pv ← I_pv
    P*_pv ← P_pv
    return I_ref
```

3 Common system architectures

For usual household or commercial applications, a group of modules is required to attend the power needs. The architectures for dealing with the issues of multiple modules may differ in number of converters, sensors, microprocessors, power levels in each converter and MPPT efficiency and efficacy, specially under non-uniform conditions. Next, we explore some characteristics of the most common (central converter) topology and the rising micro-converter architecture.

For all architectures presented in the sequence, it is assumed the same control technique for a fair comparison. For illustration purposes, we consider the switching rule design from (Dezuo et al., 2014), which only requires the measurement of a current I_L on the converter for the control.

3.1 Central converter

The central converter topology consists of a single converter that centralizes the power flow, as shown in Figure 2. It typically needs to support higher power flows and higher voltage levels.

In this architecture, all modules are interconnected in a single PV array. By rearranging the interconnections in different manners, as shown in Figure 3, different voltage and current levels are expected on the output of the array.

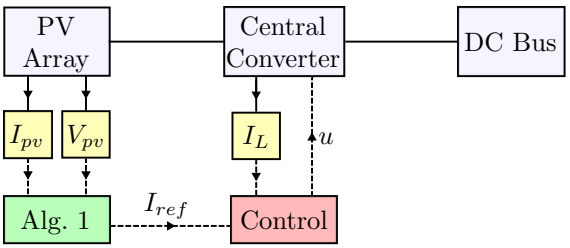

Figure 2: Typical central converter architecture. The yellow blocks represent sensors.

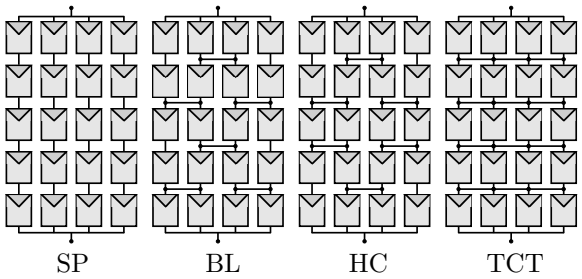

Figure 3: Common array interconnections: Series-Parallel (SP), Bridge-Link (BL), Honey Comb (HC) and Total-Cross-Tied (TCT). Adapted from (Vijayalekshmy et al., 2014).

The characteristic curves for the array are a combination of the individual characteristics from Figure 1. For this reason, different interconnections result in different I-V characteristics for the array under non-uniform conditions. In this condition, multiple maxima are expected for the $P-I$ curve and more complex MPPT strategies must be employed to avoid being stuck in a smaller local maximum. More details about the effects of different interconnections can be found in (Squersato et al., 2019).

Although, even with the interconnection that provides the best global maximum and a MPPT able to reach it, this maximum is smaller than the supreme maximum (P_{sup}) that could be generated if all the MPP of each module (P_{max}) were attained simultaneously. Notice that it is not possible as the converter can only regulate the characteristics of the array and not of individual modules. Thus this topology may have considerable power losses for different panels or operating conditions.

3.2 Micro-converters

Micro-converter architectures are a solution for obtaining the most power possible (P_{sup}) by having a converter regulating the operation point of each module to its MPP. Let us consider the DC-DC micro-converter architecture presented in Figure 4 (York Jr, 2013) for a number of modules (M) equals to two. Notice that the strategy is the same as for central converters, just repeated for each module individually, which leads the number of all system components to be multiplied by M. As the power flow is restricted to the generation of one module, simpler and less expensive low-power converters can be used. Nevertheless, it yields a higher initial investment, specially for sensors and microprocessors.

The output of the DC-DC converters can be interconnected in series/parallel to the DC Bus (a battery or a DC link to an inverter). In the parallel interconnection the control of each converter is decoupled, as all converters receive the same DC Bus voltage, and thus simpler. Although, it requires higher voltage gains from the modules to the DC Bus (Cao et al., 2015). This is necessary for the inverters to construct the higher voltage levels of the grid. On the other hand, series interconnections are more difficult to control, as the voltages of both sides of the converter are variable and dependent of the other converter outputs.

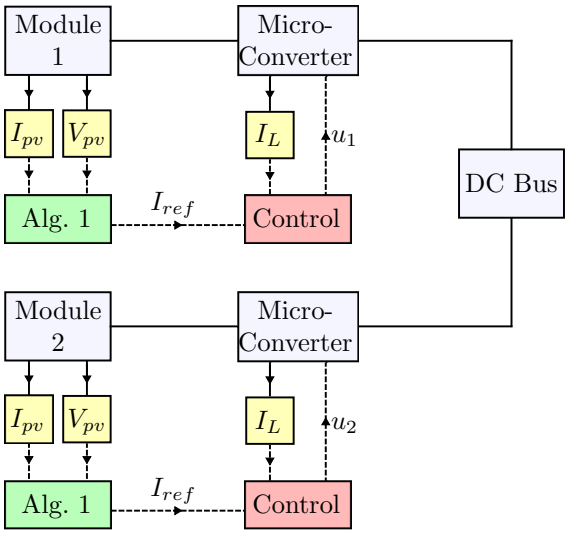

Figure 4: Typical micro-converter architecture.

4 Proposed architecture

In this paper we are interested in combining the advantages of generating P_{sup} with lower initial costs. For this purpose, we propose a decentralized DC-DC micro-converter architecture with centralized sensing and processing.

The main idea is to adapt the MPPT P&O strategy to perform its function by measuring only the current flowing through the DC Bus (I_B), as proposed in Figure 5. This represents an enormous reduction on the number of sensors needed for MPPT compared to the traditional micro-converter architecture from Section 3.2, which has both I_{pv} and V_{pv} measured M times. It is even less than the two sensors required for MPPT in the central converter architecture.

In order for that to work, the following issues must be addressed. **(i)** The current I_B is, for most converter topologies, a pulsing signal; **(ii)** How to determine which module must have its operation

point adjusted based on a common signal? **(iii)** If not updating simultaneously, then when to stop updating a panel to start another? **(iv)** How to differentiate the effects of a module being updated from a module going into shading, for instance, with no direct measurements?

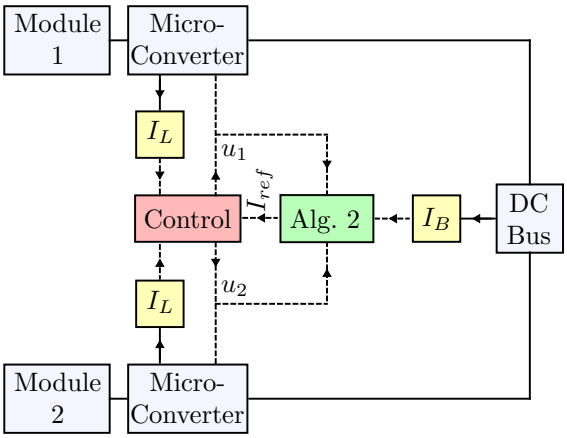

Figure 5: Proposed architecture.

First of all, let us consider the DC Bus voltage V_B to be constant or to have a very slow dynamics compared to the dynamics of I_B. In this case, the power flowing to the DC Bus, $P_B = V_B I_B$, varies proportionally to I_B. This means, it is not necessary to measure V_B to make assertions about the power changes on the DC Bus. Thus, it is possible to adapt the P&O algorithm to disturb the the operation point of a panel and check if I_B increased or decreased. Note that multiple panels should not be simultaneously updated as it may result in opposite effects and no conclusion could be reached about the generation.

However, while the power generated by the panels varies continuously, the output currents of the converters are piecewise functions. For instance, consider a PV module and a Boost converter connected to the DC Bus, as shown in Figure 6. The output current of the Boost converter is zero when its internal switch is *on* and has a non-null value otherwise. Considering a micro-converter structure with multiple PV-Boost topologies connected in parallel to the DC Bus, the current I_B is the sum of each output current, therefore also piecewise. Moreover, the converters do not have a synchronized switching, preventing any conclusion about the variation of I_B.

The aforementioned issue can be easily solved by the use of a digital filter, as the moving average. The Function 1 presents the mean value of the last n samples. The algorithm is properly initialized after the number of samples (s) is greater than n, that is the window is fully populated.

Subjecting I_B to the Function 1, produces the average current value I_f, which is also related to the average power flowing to the DC Bus. Thus, we may use I_f to perform the P&O adaptation,

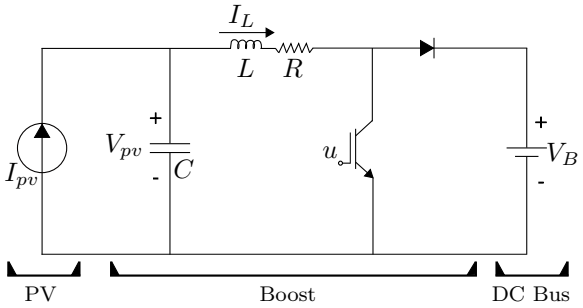

Figure 6: PV-Boost system topology.

Function 1 Digital Filter - Moving Average

Data: n
function FILTER(X)
  $s \leftarrow s + 1$
  if $s \geq n$ **then**
    $X_f \leftarrow X_f + \dfrac{X - X^*(s-n)}{n}$
  for $i \leftarrow 0$ **to** $n-1$ **do**
    $X^*(s-n+i) \leftarrow X^*(s-n+i+1)$
  $X^*(s-1) \leftarrow X$
  return X_f

as proposed in Function 2.

Function 2 Perturb PV & Observe DC Bus

Data: ΔI
function ADAPTEDP&O(I_f, I_{aux})
  if $I_f - I_f^* > 0$ **then**
    $I_{aux} \leftarrow I_{aux} + \Delta I$
    $v \leftarrow 1$
  else
    $I_{aux} \leftarrow I_{aux} - \Delta I$
    $v \leftarrow 0$
  $I_f^* \leftarrow I_f$
  return I_{aux}, v

The Function 2 returns I_{aux} as the entry of I_{ref} being updated, where I_{ref} is now a vector containing the current references for the M modules. Notice that the Function 2 also returns the binary variable v, which represents the direction of the last reference variation. By analyzing the pattern of variation of v, it is possible to detect when the MPP of a panel has been achieved and then start updating the next panel. The MPP detector presented in Function 3 has been proposed in (de Souza and Dezuo, 2019).

According to (de Souza and Dezuo, 2019), in order to characterize that there is an oscillation around the MPP avoiding false detections, especially due to sudden changes in radiation, at least four iterations of the Function 2 (P&O) are necessary. For this reason, an auxiliary variable k counts the number of iterations passed since the function has started and as soon as $k \geq 4$ one can judge the behavior pattern. For this, the behaviors of the variation v of the last four iterations

Function 3 MPP detector

```
1: function MPPDetector(v)
2:     for i ← 1 to 3 do
3:         V(i) ← V(i + 1)
4:     V(4) ← v
5:     k ← k + 1
6:     if k ≥ 4 then
7:         if V == [1 1 0 0] or
8:            V == [0 1 1 0] or
9:            V == [0 0 1 1] or
10:           V == [1 0 0 1] then
11:            f = 1
12:        else
13:            f = 0
14:    return f
```

are stored in the vector V. Such a vector operates as a movable window, always storing the v (most recent) in the last element and moving the oldest ones to the first positions. Finally, V is compared to the four patterns that characterize the MPP and, if one matches, a binary flag f is set. See (de Souza and Dezuo, 2019) for more details about the pattern identification process.

The previous strategies are enough to produce a fully functioning algorithm capable of achieving the MPP with all micro-converters. However, updating the panels in a predefined order may lead to a long times until a panel is re-updated. This is an issue when there are too many panels and the operating conditions of some panels suddenly change, causing a considerable power drop. Knowing that DC-DC power electronic converters have an input-output gain that is a function of the duty cycle (D), then variations in D may indicate variations on the I-V curve of the module.

Function 4 Duty Cycle Monitoring

```
1: Data: M
2: function DutyMonitor(u, j)
3:     for i ← 1 to M do
4:         D(i) ← Filter(u(i))
5:     ΔD ← |D − D*|
6:     i ← IndexMax(ΔD)
7:     if ΔD(i) ≥ ΔD_thr then
8:         j ← i
9:     D* ← D
10:    return j
```

Suppose a sudden change on the operating conditions. As the control keeps adjusting itself to maintain $I_{pv} = I_{ref}$, a change on the I-V curve can only reflect upon the voltage variable V_{pv}. As V_{pv} changes and V_B is constant, D must change to result in the correct gain. This change in D is what maintains the desired current in first place. Therefore, by monitoring if D suffered any variation ΔD from its previous value D^*, beyond a minimal adjustable threshold ΔD_{thr}, a sudden variation in the operating conditions has been detected. By prioritizing the MPPT for the panel that had the largest variation, it is possible to avert extensive energy losses. This proposed solution is presented in Function 4. This algorithm also contain a filter to obtain D as the average value of u, in case $u \in \{0, 1\}$ is a piecewise switching signal (depending on the output format of the controller).

The complete proposed MPPT strategy is presented in Algorithm 2. The algorithm updates the j-th panel until it reaches its maximum or until a panel with large power drop is detected and prioritized (note that the Line 9 of the Algorithm 2 overwrites j if the Duty Monitor is activated).

Algorithm 2 Proposed MPPT

```
Require: I_f, u
Ensure: I_ref
Data: ΔI, M, n, ΔD_thr
Initialize: j ← 1, s ← 0, k ← 0, v ← 0, f ← 0,
            D ← Zeros(M), D* ← Zeros(M),
            V ← Zeros(M), I*_f ← 0,
            I_ref ← Ones(M)·ΔI
1: loop
2:     I_f ← Filter(I_B)
3:     (I_ref(j), v) ← AdaptedP&O(I_f, I_ref(j))
4:     if MPPDetector(v) == 1 then
5:         if j < M then
6:             j ← j + 1
7:         else
8:             j ← 1
9:     j ← DutyMonitor(u, j)
10:    return I_ref
```

Remark 1 (Standby) *The Algorithm 2 can be further adapted to stop updating the panels that already reached their MPP and only re-update the ones that identified by the Function 4. It suffices to eliminate the Line 8 from Algorithm 2. An advantage of this is to avoid conflict in determining if a power variation was due to the P&O or to sudden changes in the operation conditions.* □

5 Numerical example

Consider a set of three PV modules parallel connected to a DC Bus through Boost microconverters. This is simply an extension of Figure 4 for the three modules case. Each PV-Boost circuit has the same topology presented in Figure 6. The parameters of the modules are the same presented in Table 1 and the parameter of the circuits can be found in Table 2. It is assumed that bypass and blocking diodes are properly installed to avoid power consumption by the modules.

In order to attest the robustness of the Algorithm 2 to non-uniform conditions, sudden vari-

Table 2: Boost micro-converter parameters

Parameters	Value
C	100μF
L	50mH
R	10mΩ
V_B	350V

ations in G affecting the j-th module were performed according to intervals shown in Table 3. It is considered that the panels are all operating with a 25°C temperature. In the same table, P_{sup} [W] represents the supreme value of the power available under such conditions, that is, the sum of the maximum powers of all modules.

Table 3: Irradiation changes simulated.

Time [s]	0-8	8-12	12-16	16-20
G_1 [W/m^2]	750	1000	1000	1000
G_2 [W/m^2]	1000	1000	750	750
G_3 [W/m^2]	1000	1000	1000	1200
P_{sup} [W]	562.4	612.6	561.3	602.3

The control technique applied is borrowed from the Example 1 of (Dezuo et al., 2014), which was designed considering the same system parameters and imposes the given reference I_{ref} to I_L. The simulations were performed using the software Matlab/Simulink considering a simulation step of 5μs. The P&O updates every $50ms$ with an amplitude $\Delta I = 0.25$A. All the moving average filters were adjusted to a $20ms$ window ($n = 4000$) and we used two filters in series to obtain an exponential smoothing effect as suggested in (Khoo and Wong, 2008).

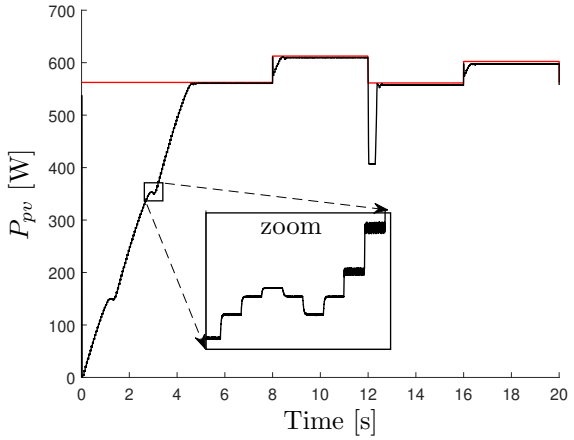

Figure 7: Total power generated (black curve) and the total power available (red lines).

The Figure 7 shows the resulting power generated over time (black curves). The supreme value P_{sup} is also shown (red lines). Note that the oscillation stops once P_{sup} is reached, inside a precision, according to the Remark 1. It is noteworthy that the system converges to the MPP of the three panels in around 4.75s. In all subsequent changes in operation conditions the system presents a fast response to reach the new MPP, which is due to the priority given for the affected panels. At 12s a panel suffered a shading for which the current operating point abruptly had its produced power zeroed (the operation point was then "out" of the new I-V curve), although it was resolved as soon as I_{ref} updated back to values on the new curve.

The module being currently updated is shown in Figure 8, where the number 0 means that no panel is being updated (the algorithm is in standby).

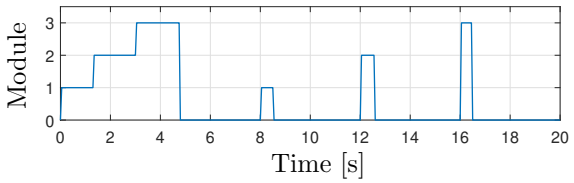

Figure 8: Module being updated.

Finally, a comparison regarding the maximum power possible between the central and micro-converter architectures is presented in Table 4. We consider the central converter with a series interconnection, as it is the most commonly installed, and the global maximum power values were obtained by using the method in (Squersato et al., 2019). Notice in Table 4 that the central converter only produces as much power as the micro-converter in case of uniform irradiation (8-12 s). For the number of sensors typically required to perform MPPT, we have 2 for the central architectures, 6 for the conventional micro-converters and only 1 for the proposed micro-converter configuration. Note that the proposed technique is superior in both characteristics.

Table 4: Architectures comparison by maximum power available for harvesting

	Time [s]			
	0-8	8-12	12-16	16-20
Central conv.				
P_{max} [W] (series)	502.0	612.6	501.6	507.0
Micro-conv.				
P_{sup} [W]	562.4	612.6	561.3	602.3

6 Concluding remarks

This paper presented a MPPT strategy for micro-converter controlled PV systems based on measuring only the DC Bus current. Thus, the main contribution is to reduce the number of sensors, but without losing the advantage of extracting the maximum power from all the modules for non-uniform conditions. A numerical example illustrated the efficacy of the method compared to conventional micro-converter and central converter architectures. The disadvantage of

the proposed method is the time for reaching the full power production as the panel updates cannot be simultaneous. This issue can be reduced by adding an initial non-null guess for the desired operation point, perhaps based on the STC.

Also with the purpose of avoiding accumulating energy losses over time, a technique for detecting unexpected changes on the operating conditions is also proposed. With a few changes the proposed algorithm can be adapted to stop panel updates until detecting a change. This results in less oscillation around the MPP, although it is also subject to the small steady-state error of the P&O algorithm. This standby condition of panels that reached MPP is specially useful because it reduces the chance of a panel being updated simultaneously to a change in operating conditions, which could lead the algorithm to a wrong conclusion about the update. However, if this standoff situation occurs, it will be resolved in the next iterations of the algorithm.

For future work, it would be interesting to associate the method with another MPPT technique, instead of the basic P&O, to dodge the compromise between a fast convergence to the MPP and the precision around it. Also, the spatial centralization of the controller requires more and longer communication cables between the controller and the micro-converter. Therefore, the viability of embedded and economic wireless data transmission or power line communication methods could be studied.

Acknowledgements

This study was financed in part by FAPESC through the process 873/2019, by FNDE through the *Programa de Educação Tutorial* from SESu/MEC, Brazil and by the TIM Institute through the TIM-OBMEP scholarship.

References

Cao, Z., Li, Q. and Lee, F. C. (2015). Multiphase smart converter for pv system, *2015 IEEE Applied Power Electronics Conference and Exposition (APEC)*, pp. 1736–1742.

Casaro, M. M. (2009). *Inversor trifásico de dois estágios modificado aplicado no processamento da energia solar fotovoltaica em sistemas conectados à rede elétrica*, PhD thesis, Federal University of Santa Catarina, Florianópolis, Brazil.

de Souza, C. O. and Dezuo, T. J. M. (2019). Perturba e observa adaptável para elevar a eficiência de sistemas fotovoltaicos, *Anais do 14° Simpósio Brasileiro de Automação Inteligente*, Ouro Preto, Brazil, pp. 2693–2698.

Dezuo, T. J. M., Trofino, A. and Scharlau, C. C. (2014). Switching rule design for sector-bounded nonlinear switched systems, *Proceedings of 19th International Federation of Automatic Control (IFAC) World Congress*, Cape Town, South Africa, pp. 4074–4079.

Freitas, S., Catita, C., Redweik, P. and Brito, M. C. (2015). Modelling solar potential in the urban environment: State-of-the-art review, *Renewable and Sustainable Energy Reviews* **41**: 915–931.

Khoo, M. B. C. and Wong, V. H. (2008). A double moving average control chart, *Communications in Statistics - Simulation and Computation* **37**(8): 1696–1708.

NREL (2020). Best research-cell efficiency chart, Available in: `nrel.gov/pv/cell-efficiency.html`.

Seo, G.-S., Shin, J.-W., Cho, B. and Lee, K.-C. (2014). Digitally controlled current sensorless photovoltaic micro-converter for DC distribution, *IEEE Transactions on Industrial Informatics* **10**: 117–126.

SolarPower Europe (2019). Global market outlook for photovoltaics 2019-2023, Available in: `http://solarpowereurope.org`.

Soualmia, A. and Chenni, R. (2016). A survey of maximum peak power tracking techniques used in photovoltaic power systems, *IEEE Future Technologies Conference 2016* pp. 430–443.

Squersato, I., Lunardi, H. C. and Dezuo, T. J. M. (2019). Algoritmo para simulação e análise de arranjos fotovoltaicos reconfiguráveis sob condições não uniformes, *Anais do 14° Simpósio Brasileiro de Automação Inteligente*, Ouro Preto, Brazil, pp. 1783–1788.

Torres, I. C. (2016). *Análise do desempenho operacional de sistemas fotovoltaicos de diferentes tecnologias em clima tropical - estudo de caso: sistema fotovoltaico conectado à rede*, Master's thesis, Federal University of Pernambuco, Recife, Brazil.

Vijayalekshmy, S., Bindu, G. R. and Iyer, S. R. (2014). Estimation of power losses in photovoltaic array configurations under moving cloud conditions, *2014 4th International Conference on Advances in Computing and Communications*, pp. 366–369.

York Jr, J. B. (2013). *An Isolated Micro-Converter for Next-Generation Photovoltaic Infrastructure*, PhD thesis, Virginia Polytechnic Institute and State University, Blacksburg, USA.